Conclusion: We have successfully demonstrated our integration technology based on SAG with the realisation of a MWL showing stable single passband CW laser operation for all eight channels.

Acknowledgment: The authors acknowledge the European Commission for partial support through project ACTS AC332 (APEX). T. Van Caenegem and D. Van Thourhout acknowledge the Flemish IWT for a doctoral grant.

2 January 2001
Electronics Letters Online No: 20010188
DOI: 10.1049/el:20010188

T. Van Caenegem, D. Van Thourhout, M. Galarza, S. Verstuyft, I. Moerman, P. Van Daele, R. Baets and P. Demeester (*IMEC - University Ghent, Department of Information Technology (INTEC), St.-Pietersnieuwstraat 41, B-9000 Gent, Belgium*)

E-mail: tcaen@intec.rug.ac.be

C.G.P. Herben, X.J.M. Leijtens and M.K. Smit (*Photonic Integrated Circuits Group, Delft University of Technology, The Netherlands*)

References

1 VAN THOURHOUT, D., DE MERLIER, J., VAN CAENEGEM, T., VANWASSENHOVE, L., MOERMAN, I., VAN DAELE, P., HERBEN, C.G.P., LEIJTENS, X.J.M., VAN UFFELEN, J.W.M., SMIT, M.K., and BAETS, R.: 'Elimination of crosstalk in the common output amplifier of a multi-wavelength source by gain clamping'. OFC '99, February 1999, Paper ThV2

2 VAN CAENEGEM, T., MOERMAN, I., and DEMEESTER, P.: 'Selective area growth on planar masked InP substrates by metal organic vapour phase epitaxy', *Prog. Cryst. Growth Charact. Mater.*, 1997, **35**, (2-4), pp. 263–288

Optical gain-bandwidth product of vertical-cavity laser amplifiers

J. Piprek, E.S. Björlin and J.E. Bowers

Trade-off between amplifier gain and optical bandwidth is investigated in the case of novel long-wavelength vertical-cavity semiconductor optical amplifiers. In agreement with measurements, simple formulas for the gain-bandwidth product are presented. Mirror optimisation promises gain-bandwidth products in the THz range.

Vertical-cavity semiconductor optical amplifiers (VCSOAs) have recently attracted increasing interest. They are potentially low-cost alternatives to in-plane SOAs and have the inherent advantages of polarisation insensitivity, high fibre coupling efficiency, and a low noise figure. Two-dimensional arrays of VCSOAs are attractive for parallel applications. We have recently demonstrated the first VCSOA that operates at 1.3µm signal wavelength [1]. Fig. 1 shows our undoped and optically pumped device. Two AlAs/GaAs distributed Bragg reflectors (DBRs) are wafer bonded to an InP based active region which contains three stacks of seven compressively strained InAsP quantum wells placed at the three central peaks of the standing optical wave. The DBRs are 1µm apart and the effective cavity length is 2.2µm including mirror penetration depths. The quantum wells are the only layers to allow for band-to-band absorption of the 980nm pump laser beam which enters through the GaAs substrate and 25-period back mirror. The amplifier is operated in reflection mode, i.e. the front mirror is used for signal input and signal output (in transmission mode, signal output would be through the back DBR). With a 12-period front mirror, we measured up to 13dB fibre-to-fibre gain, –3.5dBm saturation output power, and 0.6nm optical bandwidth [2]. Low optical bandwidth is desirable for filter applications, whereas a larger bandwidth is needed for wavelength division multiplexing (WDM). Less pump power results in a larger bandwidth but lower gain. Owing to this trade-off, we investigated the gain-bandwidth product as the figure of merit.

The inset in Fig. 2 shows the measured gain against signal wavelength. Multiplying the –3dB optical bandwidth (Δf_R = 100GHz) with the square root of the peak amplifier gain (G =

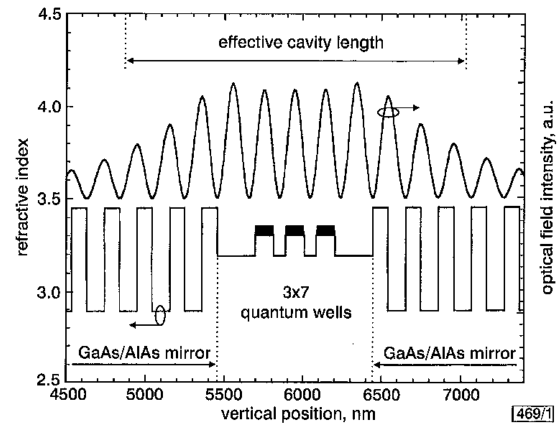

Fig. 1 *Vertical refractive index profile and standing optical wave in centre of double-fused 1.3µm vertical-cavity amplifier*

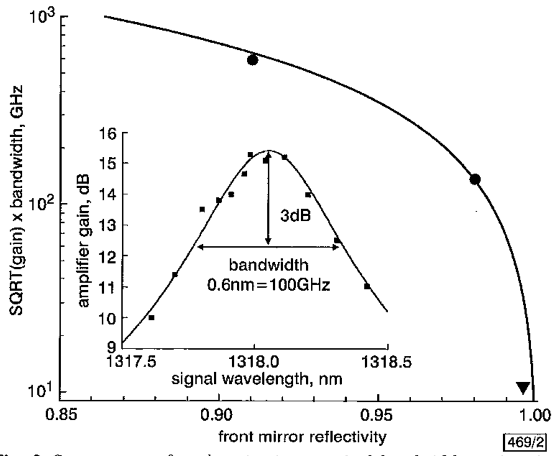

Fig. 2 *Square-root of peak gain times optical bandwidth against input mirror reflectivity*

——— as calculated
●, ▼ as measured on 3 different devices in reflection mode
● 1.3µm wavelength [1, 2]
▼ 1.5µm wavelength [4]
Inset: Measurement on device with largest gain-bandwidth product (fibre coupling losses not included)

15.4dB = 34.8) gives the gain-bandwidth product (590GHz) which is a constant for any given device (owing to the bandwidth singularity caused by the initial reflection, a minimum of ~6dB gain is required in reflection mode). For theoretical verification, we calculated the amplifier gain and optical bandwidth based on the Fabry-Perot approach [3] and derived the following simple formulas which are valid in reflection and transmission mode, respectively.

$$\Delta f_R \sqrt{G_R} = \frac{c}{2\pi n_c L_c}\left(\frac{1}{\sqrt{R_f}} - \sqrt{R_f}\right) \qquad (1)$$

$$\Delta f_T \sqrt{G_T} = \frac{c}{2\pi n_c L_c}\sqrt{\frac{(1-R_f)(1-R_b)}{\sqrt{R_f R_b}}} \qquad (2)$$

where n_c is the cavity refractive index, L_c the effective cavity length, and R_f the front and R_b the back mirror reflectivity (c is the vacuum light velocity). Remarkably, the back mirror does not affect the result in reflection mode. Fig. 2 shows the reflection mode formula against front mirror reflectivity for our device (n_c = 3.2). Dots represent measurements on three different long-wavelength VCSOAs. Our two devices for 1.3µm wavelength only differ in the front mirror reflectivity [1, 2]. In addition, we include a previously fabricated device for 1.5µm wavelength with an Si/SiO_2 front mirror and ~3.8µm effective cavity length [4]. In perfect agreement with our design formula (eqn. 1), less front mirror reflectivity results in larger gain-bandwidth products. However, stronger pumping is required to maintain constant amplifier gain with lower reflectivity. For our reflection mode case, gain-bandwidth products above 1THz can be achieved if the front mirror reflectivity is < 0.86 (Fig. 2).

Acknowledgment: This work was supported by DARPA via the Heterogeneous Optoelectronics Technology Center.

20 November 2000
Electronics Letters Online No: 20010201
DOI: 10.1049/el:20010201

J. Piprek, E.S. Björlin and J.E. Bowers (*Electrical and Computer Engineering Department, University of California, Santa Barbara, CA 93106, USA*)

E-mail: piprek@ece.ucsb.edu

References

1 BJÖRLIN, S., RIOU, B., KEATING, A., ABRAHAM, P., CHIU, Y.-J., PIPREK, J., and BOWERS, J.: '1.3μm vertical-cavity amplifier', *IEEE Photonics Technol. Lett.*, 2000, **12**, pp. 951–953

2 BJÖRLIN, S., RIOU, B., ABRAHAM, P., PIPREK, J., CHIU, Y.-J., BLACK, K.A., KEATING, A., and BOWERS, J.: 'Long-wavelength vertical-cavity semiconductor amplifiers', to be published in *IEEE J. Quantum Electron.*, 2001, **37**

3 GHAFOURI-SHIRAZ, H.: 'Semiconductor optical amplifiers' (Wiley, New York, 1995)

4 LEWEN, R., STREUBEL, K., KARLSSON, A., and RAPP, S.: 'Experimental demostration of a multifunctional long-wavelength vertical-cavity amplifier-detector', *IEEE Photonics Technol. Lett.*, 1998, **10**, pp. 1067–1069

Wide bandwidth of over 50GHz travelling-wave electrode electroabsorption modulator integrated DFB lasers

Y. Akage, K. Kawano, S. Oku, R. Iga, H. Okamoto, Y. Miyamoto and H. Takeuchi

A travelling-wave electrode electroabsorption modulator integrated distributed feedback laser to overcome the CR-induced bandwidth limitation is developed. A bandwidth much wider than 50GHz is achieved. A 40Gbit/s eye-diagram is successfully observed. The device has a potentiality for future 100Gbit/s transmission.

Introduction: An electroabsorption modulator integrated distributed feedback laser (EA-DFB) is a key component in high-capacity information networks. EA-DFBs have been widely used in practical systems, and 40Gbit/s operation of an EA-DFB has been reported [1]. However, much wider bandwidths will be required, and the bandwidth limitation due to device capacitance should be overcome, especially when the bit rate exceeds 40Gbit/s. We propose, for the first time, an EA-DFB that has a travelling-wave electrode in the EA modulator section [2, 3] to overcome the limitation. The travelling-wave electrode electroabsorption modulator integrated DFB laser (TW-EADFB) exhibits a bandwidth much wider than 50GHz and a 40Gbit/s eye-diagram.

Device structure: Fig. 1 is a schematic diagram of the TW-EADFB. This device was fabricated on an Fe-doped semi-insulating InP substrate to form a co-planar feeding electrode. The InGaAsP/InGaAsP-MQW absorption layer of the TW-EA modulator and the MQW active layer of the DFB laser were monolithically integrated by a butt-joint technique. After the 2μm-width stripes were formed by using a CH_4/H_2 reactive ion etching technique, both devices were buried with Fe-doped semi-insulating InP. The co-planar waveguide travelling-wave electrode was formed in the modulator section. The lengths of the DFB laser and the EA modulator were 450 and 225μm, respectively.

Characteristics: Fig. 2 shows the static characteristics of the DFB laser and the TW-EA modulator. The lasing wavelength of the DFB laser was 1552nm and the optical output power was ~20mW at a laser current of 100mA when the TW-EA circuit was open. The differential resistance of the DFB laser was ~6Ω. The extinction ratio of the TW-EA modulator was ~21dB at a bias of –3V. These static characteristics are almost the same as those of the conventional EA-DFB on an *n*-InP substrate with a lumped-element electrode in the EA modulator section.

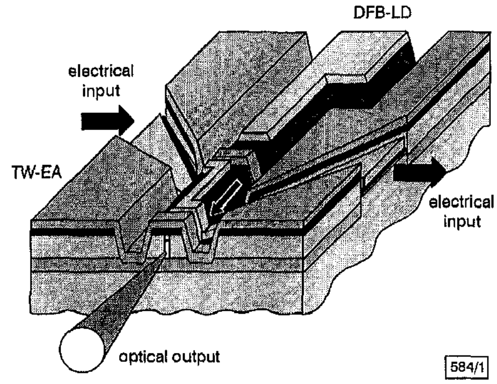

Fig. 1 *Schematic diagram of TW-EADFB*

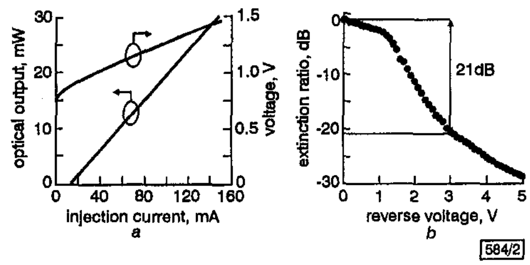

Fig. 2 *Static characteristics of DFB laser and TW-EA modulator*
a DFB laser
b TW-EA modulator

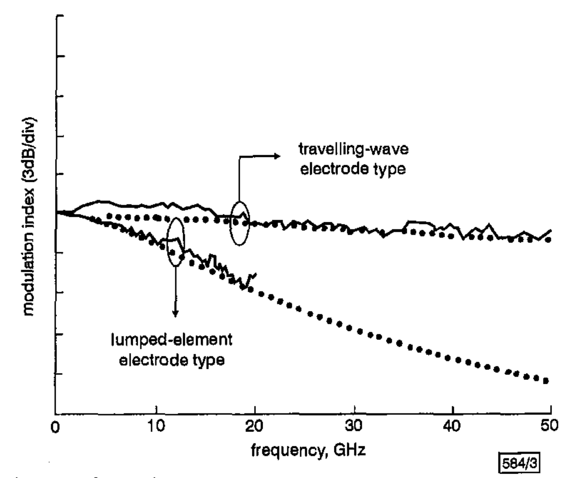

Fig. 3 *Small signal frequency response of TW-EADFB*
——— experiment
·········· simulation

Fig. 3 shows the measured small signal frequency response of the TW-EADFB. As shown in this Figure, the electrical 3dB-down bandwidth exceeds 50GHz. The bandwidth is expected to be ~70GHz from our numerical simulation. By optimising the device structure, the bandwidth of the TW-EADFB can be widened to > 100GHz. As a reference, the response of the conventional EA-DFB with a lumped-element electrode, which has the same EA modulator length, is also plotted in Fig. 3. Compared with the conventional EA-DFB, the frequency response of the TW-EADFB falls much more gradually. When the microwave signal was fed from the opposite electrode, the electrical signal propagated opposite to the direction of the light from the DFB laser. As